

Superconductivity in MgB_2 doped with Ti and C

R. H. T. Wilke^{†‡}, S. L. Bud'ko^{†‡}, P. C. Canfield^{†‡},

M. J. Kramer[‡], Y. Q. Wu[‡], and D. K. Finnemore^{†‡*}

[†]*Ames Laboratory and* [‡]*Department of Physics and Astronomy*

Iowa State University, Ames, IA 50011

R. J. Suplinskas and J. V. Marzik

Specialty Materials, Inc., 1449 Middlesex Street, Lowell, MA 01851

S. T. Hannahs

National High Magnetic Field Laboratory, Florida State University

1800 E. Paul Dirac Drive, Tallahassee, FL 32310

(Dated: March 23, 2022)

Abstract

Measurements of the superconducting upper critical field, H_{c2} , and critical current density, J_c , have been carried out for MgB_2 doped with Ti and/or C in order to explore the problems encountered if these dopants are used to enhance the superconducting performance. Carbon replaces boron on the MgB_2 lattice and apparently shortens the electronic mean free path of MgB_2 and raising H_{c2} . Titanium forms precipitates of either TiB or TiB_2 that enhance the flux pinning and raise J_c . Most of these precipitates are intra-granular in the MgB_2 phase. For samples containing both C and Ti doping, the C appears to still replace B in the MgB_2 lattice and the Ti precipitates out as a boride. If approximately 0.5% Ti and approximately 2% C are co-deposited with B to form doped boron fibers and these fibers are in turn reacted in Mg vapor to form doped MgB_2 , the resulting superconductor has $\mu_0 H_{c2}(T=0) \sim 25\ T$ and $J_c \sim 10,000\ A/cm^2$ at 5 K and 2.2 T.

PACS numbers: 74.25.Bt, 74.25.Fy, 74.25.Ha

*Electronic address: finnemor@ameslab.gov

I. INTRODUCTION

The performance of MgB_2 superconducting materials[1] can be greatly enhanced by the addition of small amounts of carbon that will raise the upper critical magnetic field, H_{c2} , [2] and the critical current density, J_c . [3] Point defects like carbon that substitute for boron in the host lattice have been shown to raise $\mu_o H_{c2}(T = 0)$ from 16 T in pure MgB_2 to 32 T for a carbon level of $\sim 4\%$. [4] At higher carbon contents, $\mu_o H_{c2}$ rises more slowly and eventually drops to about 25 T at $\sim 10\%$ carbon. [5, 6] Several different precipitate phases have been used to form small pinning sites in the MgB_2 lattice. For example, SiC , [7] YB_4 , [8], TiB_2 [9] and $MgSi_2$ [10] have been added and show a rise of J_c into the range of 10^6 A/cm² at 10 K and self field with about 5% precipitate additions. In many of these experiments, either a powder-in-tube (*PIT*) process or a pressed and sintered pellet method have been used to form the precipitates for the synthesis.

In a different approach to sample preparation, a chemical vapor deposition, *CVD*, method [11] can be used to co-deposit *B* together with a doping element to form long lengths of carbon doped boron fiber. [4] Subsequent heat treatment in *Mg* vapor transforms the doped boron into doped MgB_2 . [4] Both the *CVD* and powder methods have advantages. The advantage of powder methods is that the diffusion lengths are comparable to the powder size giving relatively low reaction temperatures and short reaction times. The advantage of co-depositing the impurity with the *B* in a *CVD* process is that the impurity is mixed with the *B* on an atomic scale. Both *Ti* [3] and *C* [4] separately have been successfully doped into MgB_2 using these *CVD* methods.

The purpose of the work reported here is to study the combined *C* and *Ti* doping of MgB_2 to determine whether samples can be prepared with the combined benefits of both dopants, raising $\mu_o H_{c2}$ to the range of 30 T and raising J_c values to the range of 10^4 A/cm² at 20 K and 5 T. Two specific questions need to be addressed. Does the addition of *Ti* to the *C*-doped MgB_2 samples reported earlier, [4] reduce the amount of *C* in the MgB_2 lattice, possibly by forming *TiC* precipitates? In the presence of *C*, can the *Ti* precipitate size be maintained at ~ 5 nm for high J_c performance?

II. EXPERIMENTAL

Long lengths of doped boron fiber are prepared in a *CVD* apparatus similar to that used for commercial boron filament production.[11] All of the materials reported here were deposited on a *W* fiber with an initial diameter of about $15\mu m$. The *W* enters the reaction chamber moving at a few *cm/s* through a *Hg* seal into a long glass tube containing flowing H_2 , BCl_3 , CH_4 , and $TiCl_4$. For *Ti* doping, H_2 is bubbled through liquid $TiCl_4$ to provide $TiCl_4$ molecules in the gas stream. Typically the BCl_3 flow rate was 3 l/min with the CH_4 and $TiCl_4$ flow rates adjusted for the desired doping levels. The diameter of the exiting doped *B* fibers were in the $75\mu m$ to $100\mu m$ range. The doped *B* fibers were cut to lengths of $\sim 3\text{ cm}$ and placed in a *Ta* tube with a *Mg* to *B* ratio of 1 : 1. The *Ta* was welded shut, sealed in a quartz tube, and heat treated in a box furnace for appropriate periods. Upon removal from the furnace, ampoules were quenched in water. Resistivity measurements are made by a four contact method using silver epoxy to make the electrical contacts. A Quantum Design *PPMS* system was used to make resistivity vs temperature, ρ vs. T , measurements up to 14 T . At higher fields, ρ vs. H measurements are made in a 32.5 T copper coil magnet at the National High Magnetic Field Laboratory at Florida State University. Magnetization measurements were made in a Quantum Design SQUID magnetometer with a magnetic field range of 5.5 T and J_c was determined from the magnetization hysteresis using the Bean Model for cylindrical shell samples.[3] A Philips CM30 transmission electron microscope (*TEM*) was employed for the microstructure characterization. Samples for the *TEM* were made using a crush-flow technique.

III. *Ti*-DOPING ONLY

In an earlier publication,[12] we investigated a series of *Ti*-doped MgB_2 samples that were deposited on a commercial carbon coated *SiC* fiber substrate with a diameter of approximately $80\mu m$ instead of the $15\mu m$ diameter *W* substrate used here. The doped- MgB_2 layers ranged from about $4\mu m$ to $10\mu m$ thick. Flux pinning was excellent and gave J_c over $10,000\text{ A/cm}^2$ at 25 K and 1.3 T for a sample with an average doping of about $9\%Ti$. [3] Unfortunately, there were problems with this approach to sample preparation. First, the diffusion of *Mg* into the *B* caused swelling and the MgB_2 pulled away from the substrate.

Second, the presence of a carbon coated substrate made the amount of C in the specimen uncertain. In addition, these samples had a rather inhomogeneous Ti distribution. There was a high Ti level near the SiC core and near the outer surface of the fiber.[3] Transmission electron microscope (TEM) observations for one of these samples that had been reacted for 2 h at $950^\circ C$ are shown in Fig. 1a. Results reveal a random distribution of precipitates scattered through the grain, ranging in size from 1 nm to 20 nm with a spacing about 5 times as large. Energy dispersive spectroscopy for a large portion of the grain in Fig. 1a, revealed that the Ti/Mg ratio was $\sim 5\%$. Selected area diffraction taken along the c-axis showed the prominent hexagonal pattern of MgB_2 with additional powder pattern rings arising from the titanium boride precipitates. The beam was then tipped off axis to show the rings more prominently. Indexing the rings revealed that the precipitates were TiB rather than TiB_2 . These results differ from those found by Zhao and coworkers.[13] They found that samples prepared by mixing powders of Mg , Ti , and B and reacting gave TiB_2 precipitates on the MgB_2 grain boundaries. This illustrates that different sample preparation methods can yield different types and locations of the precipitates. Both the precipitation of TiB throughout the grains[12] and precipitation of TiB_2 on the grain boundaries[13] seem to give enhanced flux pinning.

Samples with 15 μm diameter tungsten cores were prepared using three different $TiCl_4$ flow rates in the CVD reactor, 0.42 cc/min, 1.26 cc/min and 2.9 cc/min. After the CVD deposition, the fibers were reacted in Mg vapor to form Ti -doped MgB_2 . Energy dispersive spectra (EDS) in a scanning electron microscope (SEM) was used to probe the uniformity of Ti distribution across the superconducting fiber and to measure the Ti to Mg ratio, $[Ti]/[Ti + Mg]$. Line scans in various regions of the sample show that the Ti level was uniform to about 10% of the average value. Multiple point scans and area scans in the EDS give average values of the $[Ti]/[Ti + Mg]$ ratio, shown in Fig. 2 indicating that the percent Ti is roughly linearly related to the flow rate in the reaction chamber. Point scans, line scans, and large area raster scans were used for analysis. The large area raster scan shown by the open squares on Fig. 2 comprises the most data and are probably the most accurate measure of the Ti content. These three flow rates of 0.42 cc/min, 1.26 cc/min, and 2.9 cc/min, give 0.3%, 0.5% and 1.6% respectively for the $[Ti]/[Ti + Mg]$ ratio.

Because these Ti doped samples were deposited on a 15 μm diameter W wire and had a 76 μm outer diameter, these fibers require much longer times or higher temperatures to

fully form the MgB_2 phase than the 4 to 10 μm B layers of the earlier work.[3] Therefore, temperatures of 1000 to 1200°C were often used. A sample with 0.5% Ti reacted for 72 h at 1000°C were found to be 95% reacted using polarized light in an optical microscope. A TEM micrograph of this sample, Fig. 1b, shows precipitates that are much larger than in Fig. 1a. In this figure, the sweeping shaded areas arise from the underlying holey carbon support. In this micrograph, the beam has been tilted to emphasize areas of dense dislocations as shown, for example, in the top center of the micrograph. Many of the precipitates were 50 to 200 nm in diameter. Selected area diffraction indicated the precipitates were TiB_2 and had c-axes coaxial with the MgB_2 grains in which they were imbedded. For a sample with 0.5% Ti plus 2.1% C , the sample was fully reacted after 48 h at 1200°C and shows the 20 to 100 nm diameter precipitates of Fig. 1c. Again the large precipitates here are TiB_2 with the c-axis parallel to the c-axis of the MgB_2 grain in which it is imbedded.

Another series of samples having 0.3%, 0.5% and 1.6% Ti were all reacted at 1100°C for 48 h and studied in the TEM . For 0.3% Ti , the precipitate size is less than 50 nm and widely spaced. For 0.5% Ti , the precipitate size ranges from 20 to 80 nm . For 1.6% Ti , the precipitate size ranges from 20 to 100 nm and the density of precipitates is correspondingly higher. All of these samples show J_c values higher than pure B , but lower than shown by the sample of Fig. 1a.

Magnetization data, shown in Fig. 3, indicate that the suppression of T_c with Ti doping depends on the temperature at which the MgB_2 forms. Samples reacted at 1000°C for 72 h have magnetization curves similar to pure MgB_2 except that they are shifted to lower temperature by about 1 K . The 0.3% Ti and 1.6% Ti are nearly identical whereas the 0.5% Ti sample is a bit lower. The depression is not monotonic in Ti content, and the results on Fig. 3 probably represent true scatter in the data. The cause of the suppression in T_c is not understood. If the Ti all precipitates as TiB or TiB_2 and no Ti is incorporated in the MgB_2 lattice, then it might be expected that the suppression of T_c might be rather small and arise from lattice strains induced by the precipitates or other defects in the MgB_2 . It is also possible that some Ti atoms replace Mg in the MgB_2 lattice and reduce the superconducting interaction in that way. Further study is going to be needed to determine which variables contribute to this suppression in T_c .

At 1100°C for 48 h , the suppression of T_c behavior in Fig. 3b is similar to Fig. 3a except that the downward shift of T_c is somewhat larger. At 1200°C for 24 h , shown in Fig. 3c,

the suppression of T_c is very large and increases monotonically with Ti content. Because the $4\pi M$ vs. T curves are not always monotonic in the Ti content, a new series of samples were made at $1100^\circ C$ to check reproducibility. The data for the two sets of samples with the same Ti content differed by as much as 0.5 K . With these large TiB_2 precipitates, there are some as yet uncontrolled parameters.

An X-ray study of the shift in the MgB_2 a-axis lattice constant was undertaken to look for a connection between the lattice constant and the amount of impurity. For the case of carbon,[4] the a-axis lattice constant contracts linearly with increasing C , as shown by Fig. 4, while the c-axis remains essentially unchanged as reported by several authors.[4] For the case of Ti , the picture is more complicated. As shown in Fig. 4, the a-axis contracts with increasing Ti , but there is considerable scatter in the data and the amount of change in the a-axis may depend on the temperature at which the MgB_2 is formed. An additional sample with 4.7 cc/min flow rate of $TiCl_4$ ($2.4\%Ti$) and reacted at $1200^\circ C$ for 12 h is shown by the open square of Fig. 4. The apparent flat region of the a-axis lattice parameter between 0.5% and $2.4\% Ti$ as shown by the open squares would appear to indicate that a solubility limit has been reached for Ti in MgB_2 at about $0.5\% Ti$.

For the case of Ti additions only, samples with an $1100^\circ C$ for 48 h reaction temperature are used to illustrate the changes in superconducting properties. The values of H_{c2} measured up to 9 T for the three different Ti concentrations are slightly lower than for pure MgB_2 as shown on Fig. 5. As was found for values of $4\pi M$ vs. T curves in Fig. 3b, the $0.5\% Ti$ sample has the largest suppression of T_c and the largest suppression of H_{c2} .

As shown by Fig. 6, the J_c values at 20 K for these three Ti concentrations are enhanced by about a factor of 10 at fields, up to about 1.5 T . There is very little difference in J_c as the Ti level is raised from $0.3\%Ti$ to about $1.6\%Ti$. Values of J_c drop through 1 kA/cm^2 at about 1.5 T even though $\mu_o H_{c2}$ is above 6 T at 20 K for these three samples as shown in Fig. 5.

IV. COMBINED Ti AND C DOPING

All the samples reported here for the combined doping were reacted at $1200^\circ C$ to ensure full conversion to the MgB_2 phase. The C content is determined from the CH_4 flow rate in the CVD chamber and previous results.[4] For a sample with $0.5\%Ti$ plus $2.1\%C$ shown in

Fig. 1c, the precipitates are 20 to 100 *nm* in diameter and selected area diffraction shows the precipitates to be TiB_2 with the c-axis parallel to the c-axis of the MgB_2 grain in which they are imbedded. In this micrograph, the beam is tilted so that the dislocations are not so apparent, but they are there. These precipitates of Fig. 1c are similar to those in Fig. 1b, but in contrast to the TiB precipitates of Fig. 1a.

An X-ray analysis of the combined Ti and C doping is illustrated in Fig. 7. The c-axis lattice parameter from the (002) peak essentially does not change with Ti and C addition. The a-axis lattice parameter contracts in a regular way as shown by the (110) peak of Fig. 7. The 0.5% Ti -only peak moves to higher angle than the pure MgB_2 peak by about 0.11 degree as shown by the heavy dotted line. The 2.1% C -only peak shifts out from the pure MgB_2 peak by about 0.22 degree as shown by the light dotted line. And, the 0.5% Ti +2.1% C peak shifts out from the pure MgB_2 peak by about 0.29 degree as shown by the heavy solid line. Roughly speaking, the decrease in a-axis lattice parameter is additive for Ti and C doping at this level.

As was reported earlier,[4] the $4\pi M$ *vs.* T curves and the resulting T_c values are depressed monotonically with increasing C content as shown by the open squares and solid circles of Fig. 8. If an additional 0.5% Ti is added to each of these C concentrations, the combined suppression of T_c is roughly additive. As shown in Fig. 8, the addition of 2.1% C to MgB_2 suppressed T_c by about 2 K and the addition of 2.1% C plus 0.5% Ti suppressed T_c by about 6 K .

Values of $\mu_o H_{c2}$ in samples with the combined doping shown in Fig. 9 by the open circles are very similar to values for C doping only reported previously[4] as shown by the solid symbols. The solid triangles were taken with R *vs.* T measurements and the solid circles were taken at the National High Magnetic Field Laboratory as R *vs.* H measurements. For the combined Ti and C doped samples there was considerable rounding at the high field end of the R *vs.* H transitions. The two open circles represent two different definitions of $\mu_o H_{c2}$, the lower being a linear extrapolation of the long linear region of R *vs.* H up to the normal state, and the upper open circle being the field where the resistivity reaches the normal state value within the noise. The addition of a few percent C to the Ti doped samples substantially raises $\mu_o H_{c2}$ (open circles) to values comparable to values for carbon only (solid symbols).

Values of J_c for a series of samples reacted at 1200°C are shown in Fig. 10. For the

combined 2.1% C + 0.5% Ti sample at 5 K , the J_c curve crosses 1 kA/cm^2 at about 3.2 T shown by the solid circles. The 1.1% C + 0.5% Ti sample at 5 K crosses 1 kA/cm^2 at 2.6 T , as shown by the open circles. The 0.5% Ti only sample has the highest low field J_c values and crosses 1 kA/cm^2 at 2.3 T . A pure MgB_2 sample at measured at 5 K is shown by the solid squares. It is not shown here, but the the combined 2.1% C + 0.5% Ti sample at 20 K , the J_c curve crosses 1 kA/cm^2 at about 1.5 T .

To summarize, the addition of C to raise H_{c2} and the addition of Ti to form precipitate pinning centers are roughly independent of one another for the samples reported here. Carbon doped MgB_2 shows a rapid rise in $\mu_o H_{c2}(T = 0)$ from 16 T for pure MgB_2 to 25 T for $\sim 2.1\%$ added carbon. With both 2.1% C and 0.5% Ti the sample retains a $\mu_o H_{c2}(T = 0)$ of $\sim 25\text{ T}$ and no evidence for the formation of TiC was seen. The addition of Ti enhances J_c substantially in the magnetic field range of 2.5 to 3.5 T , as shown in Fig. 10.

Much work needs to be done to optimize the the C and Ti levels and the processing to raise J_c at high fields. For low reaction temperatures and short times to form the MgB_2 phase, TEM data show that the precipitates are intra-granular and randomly oriented particles ranging in size from 1 to 20 nm . For higher reaction temperatures in the range from 1000 to 1200°C, the precipitates are much larger. The precipitates are usually intra-granular TiB_2 particles coplanar with the MgB_2 host that range from 50 nm to 200 nm in size. Coarsening of the TiB_2 precipitates at high temperatures and long times is clearly a problem. In magnetic fields from zero to 1 T , the addition of carbon to Ti -doped MgB_2 gives relatively little change in J_c , but in the 3 to 4 T range, carbon additions clearly enhance J_c . A very practical problem is that the addition of either C or Ti slows down the rate at which the B fibers transform to the MgB_2 phase. For high J_c values, it is helpful to react at low temperatures to give small MgB_2 grains and to prevent the Ti precipitate coarsening. Some method is needed to overcome these slow reaction rates, probably the use of fine powders to keep the reaction time short and the reaction temperatures low. It would be desirable to make doped boron powders so that the diffusion lengths can be much smaller and the reaction temperatures lower.

Acknowledgments

Ames Laboratory is operated for the US Department of Energy by Iowa State University under Contract No. W-7405-Eng-82. This work was supported by the Director for Energy Research, Office of Basic Energy Sciences. A portion of this work was performed at the National High Magnetic Field Laboratory, which is supported by NSF Cooperative Agreement No. DMR-0084173 and by the State of Florida.

-
- [1] Paul C. Canfield and George W. Crabtree, *Physics Today*, **56** (3), 34 (2003).
 - [2] A. Gurevich, S. Patnaik, V. Braccini, K. H. Kim, C. Mielke, X. Song, L. D. Cooley, S. D. Bu, D. M. Kim, J. H. Choi, L. J. Belenky, J. Giencke, M. K. Lee, W. Tian, X. Q. Pan, A. Siri, E. Helstrom, C. B. Eom, D. C. Larbalestier, *Supercon. Sci. Technol.* **17** (2004) 278.
 - [3] N. E. Anderson Jr., W. E. Straszheim, S. L. Bud'ko, P. C. Canfield, D. K. Finnemore, and R. J. Suplinskas, *Physica C*, **390** (2003) 11.
 - [4] R. H. T. Wilke, S. L. Bud'ko, P. C. Canfield, D. K. Finnemore, R. J. Suplinskas, and S. T. Hannahs, *Phys. Rev. Lett.*, **92** (2004) 217003.
 - [5] R. A. Ribeiro, S. L. Bud'ko, C. Petrovic, and P. C. Canfield, *Physica C* **384** 2003 227.
 - [6] Z. Holanová, J. Kacmarcik, Z. Szabo, P. Samuely, I. Sheikin, R. A. Ribeiro, S. L. Bud'ko, and P. C. Canfield, *Physica C* **404** (2004) 195.
 - [7] X. L. Wang, Q. W. Yao, J. Horvat, M. J. Qin, and S. X. Dou, *Supercond. Sci. Technol.*, **17** (2004) L21.
 - [8] J. Wang, Y. Bugoslavsky, A. Ferenov, L. Cowey, A. D. Caplin, L. F. Cohen, J. L. MacManus-Driscoll, L. D. Cooley, X. Song, and D. C. Larbalestier, *Appl. Phys. Lett.* **81** (2002) 2026.
 - [9] Y. Zhao, Y. Feng, C. H. Cheng, L. Zhou, Y. Wu, T. Machi, Y. Fudamoto, N. Koshizuka, and M. Murakami. *Appl. Phys. Lett.* **79** (2001) 1154.
 - [10] X. F. Rui, Y. Zhao, Y. Y. Xu, L. Zhang, S. F. Sun, Y. Z. Wang, and H. Zhang, *Supercond. Sci. Technol.* **17** (2004) 689.
 - [11] R. J. Suplinskas, J. V. Marzik, Boron and Silicon Carbide Filaments, in *Handbook of Reinforcements for Plastics*, J. V. Milewski and H. S. Katz (Eds.) Van Nostrand Reinhold, New York, 1987.
 - [12] D. K. Finnemore, W. E. Straszheim, S. L. Bud'ko, P. C. Canfield, N. E. Anderson, and R. J. Suplinskas, *Physica C* **385** (2003) 278.
 - [13] Y. Zhao, D. X. Huang, Y. Feng, C. H. Cheng, T. Machi, N. Koshizuka, and M. Murakami, *Appl. Phys. Lett.* **80** (2002) 1640.

FIGURE CAPTIONS

Fig. 1 *TEM* micrograph of MgB_2 with 5%*Ti* reacted $950^\circ C$ -2 *h*, *C* coated *SiC* substrate.
b) MgB_2 with 0.5%*Ti* reacted $1000^\circ C$ -72 *h*, *W* substrate. c) MgB_2 with 0.5%*Ti* + 2.1%*C* reacted $1200^\circ C$ -48 *h*, *W* substrate.

Fig. 2 Percent *Ti* in MgB_2 sample as a function of the $TiCl_4$ flow rate in the *CVD* apparatus.

Fig. 3 Magnetization transitions for 3 different *Ti* levels at a) $1000^\circ C$, b) $1100^\circ C$ and $1200^\circ C$.

Fig. 4 Comparison of change in a-axis lattice constant for both *Ti* and *C* doping.

Fig. 5 H_{c2} for MgB_2 doped with *Ti* only.

Fig. 6 Enhancement of J_c with *Ti* additions.

Fig. 7 X-ray data for the (002) and (110) peaks for pure B, 0.5% *Ti*, 2.1%*C*, and 0.5%*Ti* + 2.1%*C*.

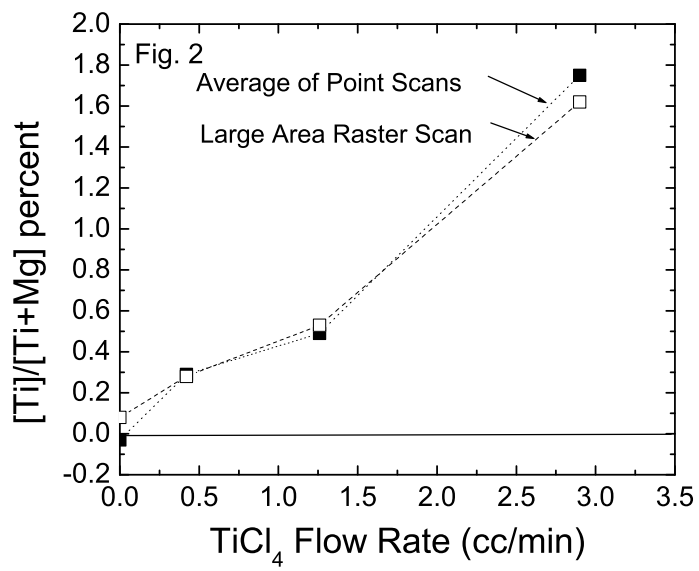
Fig. 8 Comparison of *C* + *Ti* doping with *C* only.

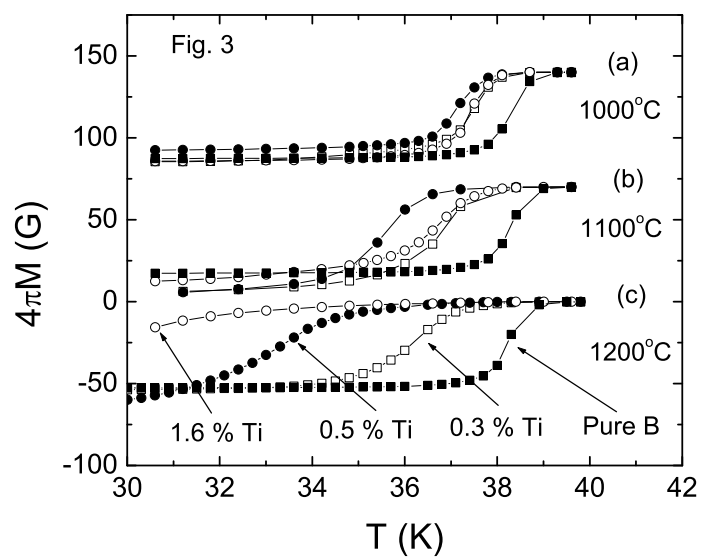
Fig. 9 H_{c2} for combined *C* + *Ti* doping (open symbols) compared to *C* only doping (solid symbols).

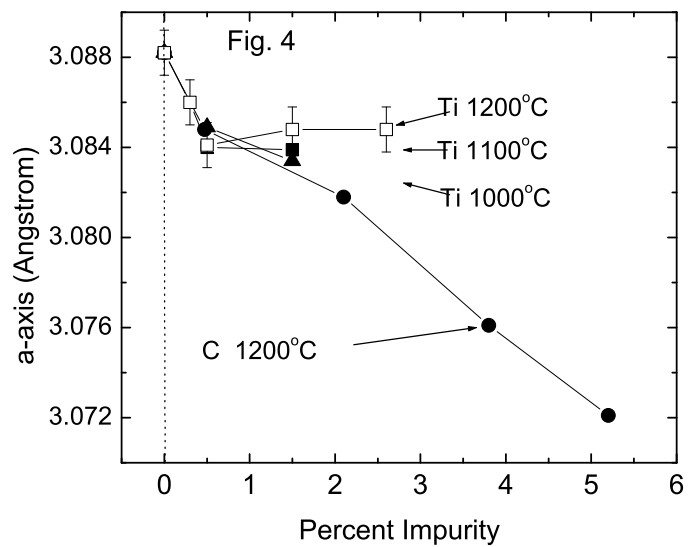
Fig. 10 Enhancement of J_c for combined *Ti* and *C* additions. The *Ti* only curve was reacted $1200^\circ C$ 12*h*. The *Ti* plus *C* samples were reacted at $1200^\circ C$ 48*h*.

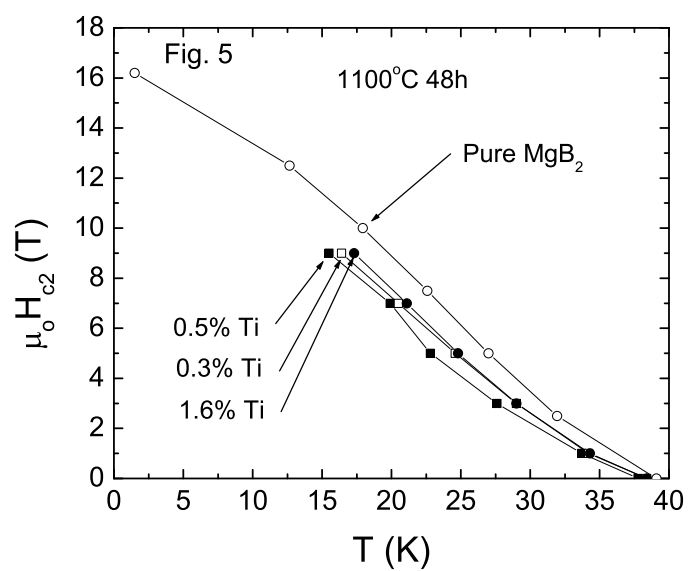
This figure "Fig1.jpg" is available in "jpg" format from:

<http://arxiv.org/ps/cond-mat/0411531v1>









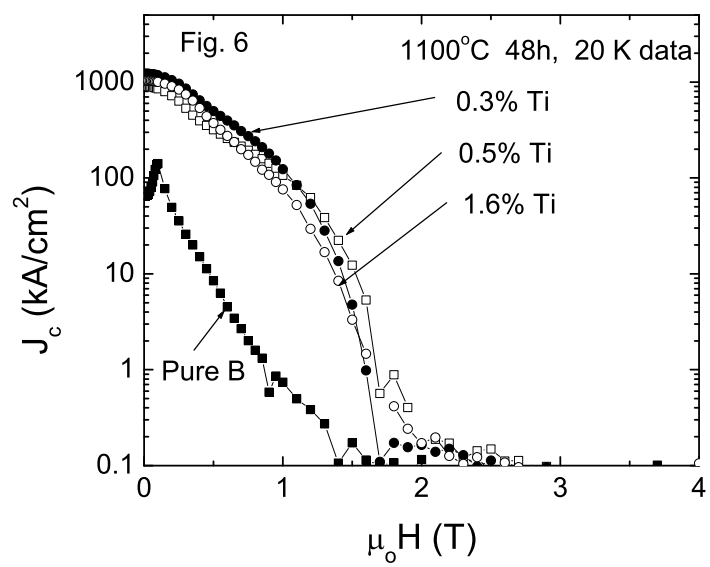


Fig. 7 1200°C

